Vol 17 No 5, May 2008
1674-1056/2008/17(05)/1784-07

Chinese Physics B

© 2008 Chin. Phys. Soc.
and IOP Publishing Ltd

Coherence-enhanced entanglement between two atoms at high temperature*

Hu Yao-Hua(胡要花), Fang Mao-Fa(方卯发)†, Jiang Chun-Lei(姜春蕾), and Zeng Ke(曾 可)

College of Physics and Information Science, Hunan Normal University, Changsha 410081, *China*

(Received 16 August 2007; revised manuscript received 5 September 2007)

This paper studies the entanglement properties in a system of two dipole–dipole coupled two-level atoms resonantly interacting with a single-mode thermal field. The results show that, when the temperature of the cavity is high enough (corresponding to the large value of the mean photon number), the entanglement is greatly enhanced due to the initial atomic coherence. These results are helpful for controlling the atomic entanglement by changing the initial parameters of the system.

Keywords: entanglement, single-mode thermal field, atomic coherence
PACC: 4250

1. Introduction

Entanglement plays a central role in many processes of quantum information theory.[1−5] Thus the issue of creating, enhancing and controlling entanglement in various composite systems has great practical importance in actual quantum information processing and has attracted much attention in theory and experiment technology.[6−16] As we all know, entanglement is intrinsically related to the superposition principle of quantum mechanics. Thus the problem of enhancing or controlling the entanglement is greatly related to the atomic coherence of population between different levels. Atomic coherence[17] can lead to many different quantum optical phenomena, such as correlated spontaneous emission laser,[18,19] spontaneous emission cancellation,[20,21] and electromagnetically induced transparency,[22] etc. In recent years, atomic coherence has been shown to play an important role in inducing, enhancing and controlling entanglement.[23−25] For example, Li *et al* showed that the atomic coherence can always induce the entanglement between two thermal fields, no matter how high the temperature of the field is.[23] In Ref.[24], Wang *et al* discovered that the two important concepts, entanglement and the atomic coherence, are closely related.

Real quantum systems will inevitably be influenced by surrounding environments, and the environment can be simulated by a thermal field. Recently, the fact that the interaction between the thermal field and quantum systems can induce entanglement has attracted much attention at the beginning of Ref.[26]. Many authors investigated the entanglement between two two-level atoms interacting with a single-mode thermal field[27−30] or with two-mode thermal field,[31] they found that two atoms become entangled by interacting with the thermal field in some specific situations. But they did not involve the influence of the atomic coherence, and the degree of the entanglement is very small especially when the value of the mean photon number is large enough (corresponding to high temperature). In this paper, we study the entanglement properties in a system of two dipole–dipole coupled two-level atoms resonantly interacting with a single-mode thermal field. The results show that, when the value of the mean photon number is very large, the dynamical entanglement is greatly enhanced due to the initial atomic coherence. These results are helpful for controlling the atomic entanglement by changing the initial parameters of the system, such as the superposition coefficients and the relative phases of the initial atomic coherent state, the coupling constant of the dipole interaction between the atoms and the mean photon number of the cavity field.

2. The model

For simplicity, we consider a system composed of two two-level atoms of the same type coupled via a

*Project supported by the National Natural Science Foundation of China (Grant No 10374025), Hunan Provincial Natural Science Foundation of China (Grant No 07JJ3013) and the Foundation of Hunan Provincial Education Department of China (Grant Nos 06A038 and 06C174).

†Corresponding author. E-mail: mffang@hunnu.edu.cn

dipole–dipole interaction. Both atoms are also interacting with a single-mode thermal field. The ground and excited states for the ith ($i = 1, 2$) atom are, respectively, denoted by $|-\rangle_i$ and $|+\rangle_i$. The cavity mode is assumed to be resonant with the atomic transition frequency. Under the rotating wave approximation, the Hamiltonian in the interaction picture is (assuming $\hbar = 1$)

$$H_{\rm I} = g\sum_{i=1,2}(a^+\sigma_i^- + a\sigma_i^+) + \Omega(\sigma_1^+\sigma_2^- + \sigma_1^-\sigma_2^+), \quad (1)$$

where $a^+(a)$ is the photon creation (annihilation) operator for the cavity field and g is the atoms–field coupling constant, $\sigma_i^- = |-\rangle_i\langle+|$ and $\sigma_i^+ = |+\rangle_i\langle-|$ are the atomic transition operators. The second term represents the dipole–dipole interaction and Ω is the coupling constant of the dipole–dipole interaction between the atoms.

Using Hamiltonian Eq.(1) and Taylor expansions of sine and cosine functions, we can obtain the analytical form of the evolution operator $U_{\rm I}(t) = \exp(-{\rm i}Ht)$ for this system in the atomic basis $|++\rangle, |+-\rangle, |-+\rangle, |--\rangle$:

$$U_{\rm I}(t) = \begin{pmatrix} U_{11} & U_{12} & U_{13} & U_{14} \\ U_{21} & U_{22} & U_{23} & U_{24} \\ U_{31} & U_{32} & U_{33} & U_{34} \\ U_{41} & U_{42} & U_{43} & U_{44} \end{pmatrix}, \quad (2)$$

where

$$\begin{aligned}
U_{11} &= 1 + 2a\frac{A}{\Lambda}a^+, \quad U_{12} = U_{13} = a\frac{B}{\Theta},\\
U_{14} &= 2a\frac{A}{\Lambda}a, \quad U_{21} = U_{31} = \frac{B}{\Theta}a^+,\\
U_{24} &= U_{34} = \frac{B}{\Theta}a, \quad U_{42} = U_{43} = a^+\frac{B}{\Theta},\\
U_{44} &= 1 + 2a^+\frac{A}{\Lambda}a, \quad U_{41} = 2a^+\frac{A}{\Lambda}a^+,\\
U_{22} &= U_{33} = \frac{\exp\left[-{\rm i}\frac{g}{2}(\alpha+\Theta)t\right]}{4\Theta}\Big\{\alpha[1-\exp({\rm i}g\Theta t)]\\
&\quad +2\Theta\exp\left[{\rm i}\frac{g}{2}(3\alpha+\Theta)t\right] + \Theta[1+\exp({\rm i}g\Theta t)]\Big\},\\
U_{23} &= U_{32} = \frac{\exp\left[-{\rm i}\frac{g}{2}(\alpha+\Theta)t\right]}{4\Theta}\Big\{\alpha[1-\exp({\rm i}g\Theta t)]\\
&\quad -2\Theta\exp\left[{\rm i}\frac{g}{2}(3\alpha+\Theta)t\right] + \Theta[1+\exp({\rm i}g\Theta t)]\Big\},\\
A &= \exp\left(-{\rm i}\frac{g}{2}\alpha t\right)\left[\cos\left(\frac{g}{2}\Theta t\right) + {\rm i}\frac{\alpha}{\Theta}\sin\left(\frac{g}{2}\Theta t\right)\right] - 1,\\
B &= \exp\left[-{\rm i}\frac{g}{2}(\alpha+\Theta)t\right][1-\exp({\rm i}g\Theta t)],\\
\alpha &= \frac{\Omega}{g}, \qquad \Lambda = 2(2a^+a+1),
\end{aligned}$$

$$\Theta = \sqrt{8(2a^+a+1)+\alpha^2}.$$

The combined atom–field system evolves for a finite time, governed by the unitary time evolution operator expressed by Eq.(2). The density operator of the system at time t is:

$$\rho(t) = U_{\rm I}(t)[\rho_{\rm f}(0)\otimes\rho_{\rm a}(0)]U_{\rm I}^+(t), \quad (3)$$

where $\rho_{\rm a}(0)$ is the initial atom–atom density operator, $\rho_{\rm f}(0) = \sum_n P_n|n\rangle\langle n|$ (photon number distribution $P_n = \bar{n}^n/(1+\bar{n})^{n+1}$) denotes the single-mode thermal radiation field with its mean photon number $\bar{n} = ({\rm e}^{\beta\hbar\omega}-1)^{-1}$, $\beta = \dfrac{1}{k_{\rm B}T}$, ω is the frequency of the field, $k_{\rm B}$ is the Boltzmann constant and T is the temperature of the cavity. Obviously, the larger the mean photon number $\bar{n}$ is, the higher the temperature is.

We are only interested in the evolution of the atoms. Hence the atom–atom density operator at any time is obtained by tracing over the field variables:

$$\begin{aligned}
\rho_{\rm a}(t) &= {\rm Tr_f}[\rho(t)]\\
&= \sum_{m,n} P_n\langle m|U_{\rm I}(t)|n\rangle\rho_{\rm a}(0)\langle n|U_{\rm I}^+(t)|m\rangle. \quad (4)
\end{aligned}$$

For a two-qubit system described by the density operator as in Eq.(4), negativity (ε) is a good measure of entanglement. Negativity is defined in terms of the negative eigenvalues of the partial transposition of the density matrix:[32–34]

$$\varepsilon = -2\sum_i \lambda_i^-, \quad (5)$$

where λ_i^- is the ith negative eigenvalue of the partial transposition of $\rho_{\rm a}(t)$. When $\varepsilon = 0$ the two atoms are separable or do not become entangled and $\varepsilon = 1$ indicates maximum entanglement between them.

3. The results

The entanglement between the two atoms (ETA) for two kinds of initial atomic coherent states is investigated when the mean photon number $\bar{n}$ is large such as $\bar{n} = 10$, $\bar{n} = 20$ and $\bar{n} = 40$, etc. First, each atom is initially a coherent superposition of different states and the two atoms are not entangled. That is, $|\Psi_1(0)\rangle = C_1|+\rangle + \sqrt{(1-C_1^2)}{\rm e}^{{\rm i}\varphi_1}|-\rangle$ and $|\Psi_2(0)\rangle = C_2|+\rangle + \sqrt{(1-C_2^2)}{\rm e}^{{\rm i}\varphi_2}|-\rangle$. Second, the

two atoms are $|\Psi(0)\rangle = C|+-\rangle + \sqrt{(1-C^2)}\mathrm{e}^{\mathrm{i}\varphi}|-+\rangle$ and entangled when $C \neq 0$ or 1. Here, C_1, C_2 and C are all real superposition coefficients and φ_1, φ_2 and φ are the relative phases.

3.1. The entanglement between the atom 1 in $|\Psi_1(0)\rangle = C_1|+\rangle + \sqrt{(1-C_1^2)}\mathrm{e}^{\mathrm{i}\varphi_1}|-\rangle$ and the atom 2 in $|\Psi_2(0)\rangle = C_2|+\rangle + \sqrt{(1-C_2^2)}\mathrm{e}^{\mathrm{i}\varphi_2}|-\rangle$

In this case, the initial density matrix for the two atoms can be written as

$$\rho_{\mathrm{a}}(0) = \begin{pmatrix} \rho_{11}(0) & \rho_{12}(0) & \rho_{13}(0) & \rho_{14}(0) \\ \rho_{12}^*(0) & \rho_{22}(0) & \rho_{23}(0) & \rho_{24}(0) \\ \rho_{13}^*(0) & \rho_{23}^*(0) & \rho_{33}(0) & \rho_{34}(0) \\ \rho_{14}^*(0) & \rho_{24}^*(0) & \rho_{34}^*(0) & \rho_{44}(0) \end{pmatrix}, \qquad (6)$$

where the matrix elements are expressed as follows:

$$\begin{aligned}
\rho_{11}(0) &= C_1^2C_2^2, \\
\rho_{13}(0) &= C_1C_2^2\sqrt{1-C_1^2}\mathrm{e}^{-\mathrm{i}\varphi_1}, \\
\rho_{12}(0) &= C_1^2C_2\sqrt{1-C_2^2}\mathrm{e}^{-\mathrm{i}\varphi_2}, \\
\rho_{14}(0) &= C_1C_2\sqrt{1-C_1^2}\sqrt{1-C_2^2}\mathrm{e}^{-\mathrm{i}(\varphi_1+\varphi_2)}, \\
\rho_{22}(0) &= C_1^2(1-C_2^2), \\
\rho_{23}(0) &= C_1C_2\sqrt{1-C_1^2}\sqrt{1-C_2^2}\mathrm{e}^{-\mathrm{i}(\varphi_1-\varphi_2)}, \\
\rho_{33}(0) &= C_2^2(1-C_1^2), \\
\rho_{24}(0) &= C_1\sqrt{1-C_1^2}(1-C_2^2)\mathrm{e}^{-\mathrm{i}\varphi_1}, \\
\rho_{34}(0) &= C_2(1-C_1^2)\sqrt{1-C_2^2}\mathrm{e}^{-\mathrm{i}\varphi_2}, \\
\rho_{44}(0) &= 1-\rho_{11}(0)-\rho_{22}(0)-\rho_{33}(0).
\end{aligned}$$

Substituting Eqs.(2) and (6) into Eq.(4), we can write down the density matrix of the two atoms at time t:

$$\rho_{\mathrm{a}}(t) = \begin{pmatrix} \rho_{11} & \rho_{12} & \rho_{13} & \rho_{14} \\ \rho_{12}^* & \rho_{22} & \rho_{23} & \rho_{24} \\ \rho_{13}^* & \rho_{23}^* & \rho_{33} & \rho_{34} \\ \rho_{14}^* & \rho_{24}^* & \rho_{34}^* & \rho_{44} \end{pmatrix}, \qquad (7)$$

where

$$\begin{aligned}
\rho_{11} &= \sum_n P_n \Big\{ [\rho_{22}(0)+\rho_{23}(0)+\rho_{32}^*(0)+\rho_{33}(0)]n\Big|\frac{B_n}{\Theta_n}\Big|^2 + \rho_{11}(0)\Big|2(n+1)\frac{A_{n+1}}{\Lambda_{n+1}}+1\Big|^2 \\
&\quad +\rho_{44}(0)4n(n-1)\Big|\frac{A_{n-1}}{\Lambda_{n-1}}\Big|^2\Big\}, \\
\rho_{12} &= \sum_n P_n \left\{ [\rho_{24}(0)+\rho_{34}(0)]n\frac{B_n}{\Theta_n}\left(\frac{B_{n-1}}{\Theta_{n-1}}\right)^* + [\rho_{12}(0)U_{22n}^*+\rho_{13}(0)U_{23n}^*]\left[2(n+1)\frac{A_{n+1}}{\Lambda_{n+1}}+1\right]\right\}, \\
\rho_{13} &= \sum_n P_n \left\{ [\rho_{24}(0)+\rho_{34}(0)]n\frac{B_n}{\Theta_n}\left(\frac{B_{n-1}}{\Theta_{n-1}}\right)^* + [\rho_{12}(0)U_{23n}^*+\rho_{13}(0)U_{22n}^*]\left[2(n+1)\frac{A_{n+1}}{\Lambda_{n+1}}+1\right]\right\}, \\
\rho_{14} &= \sum_n P_n \left\{ \rho_{14}(0)\left[2(n+1)\frac{A_{n+1}}{\Lambda_{n+1}}+1\right]\left[2n\frac{A_{n-1}}{\Lambda_{n-1}}+1\right]^*\right\}, \\
\rho_{22} &= \sum_n P_n \Big\{ \rho_{22}(0)|U_{22n}|^2 + \rho_{23}(0)U_{22n}U_{23n}^* + \rho_{23}^*(0)U_{23n}U_{22n}^* + \rho_{33}(0)|U_{23n}|^2 \\
&\quad +\rho_{11}(0)(n+1)\left|\frac{B_{n+1}}{\Theta_{n+1}}\right|^2 + \rho_{44}(0)n\left|\frac{B_{n-1}}{\Theta_{n-1}}\right|^2\Big\}, \\
\rho_{23} &= \sum_n P_n \Big\{ \rho_{22}(0)U_{22n}U_{23n}^* + \rho_{23}(0)|U_{22n}|^2 + \rho_{23}^*(0)|U_{23n}|^2 + \rho_{33}(0)U_{23n}U_{22n}^* \\
&\quad +\rho_{11}(0)(n+1)\left|\frac{B_{n+1}}{\Theta_{n+1}}\right|^2 + \rho_{44}(0)n\left|\frac{B_{n-1}}{\Theta_{n-1}}\right|^2\Big\}, \\
\rho_{24} &= \sum_n P_n \left\{ [\rho_{24}(0)U_{22n}+\rho_{34}(0)U_{23n}]\left[2n\frac{A_{n-1}}{\Lambda_{n-1}}+1\right]^* + [\rho_{12}(0)+\rho_{13}(0)](n+1)\frac{B_{n+1}}{\Theta_{n+1}}\left(\frac{B_n}{\Theta_n}\right)^*\right\}, \\
\rho_{33} &= \sum_n P_n \Big\{ \rho_{23}^*(0)U_{22n}U_{23n}^* + \rho_{23}(0)U_{23n}U_{22n}^* + \rho_{33}(0)|U_{22n}|^2 + \rho_{22}(0)|U_{23n}|^2
\end{aligned}$$

$$+\rho_{44}(0)n\left|\frac{B_{n-1}}{\Theta_{n-1}}\right|^2+\rho_{11}(0)(n+1)\left|\frac{B_{n+1}}{\Theta_{n+1}}\right|^2\Bigg\},$$

$$\rho_{34}=\sum_n P_n\left\{[\rho_{34}(0)U_{22n}+\rho_{24}(0)U_{23n}]\left[2n\frac{A_{n-1}}{\Lambda_{n-1}}+1\right]^*+[\rho_{12}(0)+\rho_{13}(0)](n+1)\frac{B_{n+1}}{\Theta_{n+1}}\left(\frac{B_n}{\Theta_n}\right)^*\right\},$$

$$\rho_{44}=1-\rho_{11}-\rho_{22}-\rho_{33},$$

and

$$U_{22n}=\frac{\exp\left[-\mathrm{i}\frac{g}{2}(\alpha+\Theta_n)t\right]}{4\Theta_n}\left\{\alpha\left[1-\exp\left(\mathrm{i}g\Theta_n t\right)\right]+2\Theta_n\exp\left[\mathrm{i}\frac{g}{2}(3\alpha+\Theta_n)t\right]+\Theta_n\left[1+\exp\left(\mathrm{i}g\Theta_n t\right)\right]\right\},$$

$$U_{23n}=\frac{\exp\left[-\mathrm{i}\frac{g}{2}(\alpha+\Theta_n)t\right]}{4\Theta_n}\left\{\alpha\left[1-\exp\left(\mathrm{i}g\Theta_n t\right)\right]-2\Theta_n\exp\left[\mathrm{i}\frac{g}{2}(3\alpha+\Theta_n)t\right]+\Theta_n\left[1+\exp\left(\mathrm{i}g\Theta_n t\right)\right]\right\},$$

$$A_n=\exp\left(-\mathrm{i}\frac{g}{2}\alpha t\right)\left[\cos\left(\frac{g}{2}\Theta_n t\right)+\mathrm{i}\frac{\alpha}{\Theta_n}\sin\left(\frac{g}{2}\Theta_n t\right)\right]-1$$

$$B_n=\exp\left[-\mathrm{i}\frac{g}{2}(\alpha+\Theta_n)t\right]\left[1-\exp(\mathrm{i}g\Theta_n t)\right]$$

$$\Lambda_n=2(2n+1),\qquad \Theta_n=\sqrt{8(2n+1)+\alpha^2}.$$

It is difficult to obtain the analytical results of the eigenvalues of the partial transposition of the system density matrix corresponding to Eq.(7). Therefore, we numerically calculate the corresponding eigenvalues, and illustrate the atom–atom negativity as a function of gt in Figs.1 and 2. The evolution of atom–atom negativity is plotted by the dotted lines for the two atoms initially in the pure initial states and by the solid lines for them initially in the coherent states.

Figure 1 shows how the mean photon number $\bar{n}$ affects the evolution of ETA when $\Omega=0.1\,g$. The values of $\bar{n}$ are 20 in Fig.1(a) and 40 in Fig.1(b), which means that the temperature of the cavity is high. Comparing the solid lines with the dotted lines in Figs.1(a) and 1(b), we note that ETA is greatly enhanced and the maximum of atom–atom negativity reaches 0.27 for $\bar{n}=20$ owing to the initial atomic coherence. With increase of the mean photon number (see Fig.1(b)), which connotes that the weight factor P_n of the single-mode thermal field becomes highly flat (which washes out the entanglement feature), the value of atom–atom negativity decreases a little for the case of the initial atomic coherent states and the maximum of ETA is 0.26, while it diminishes more when the two atoms are initially in the pure initial states and the maximum of ETA is only 0.07 (as shown in Fig.1(b)). In addition, there are lots of disentangled states of the two atoms when they are initially in product states, while the two atoms are entangled at all times except at $t=0$ for the solid line. Our results

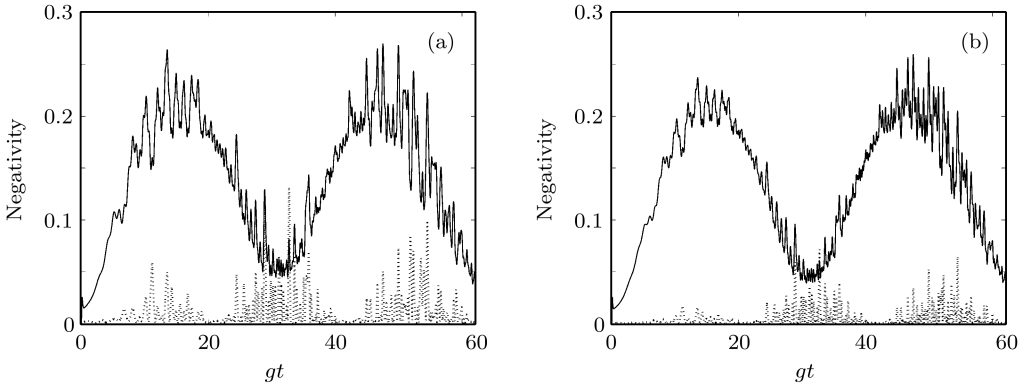


Fig.1. The evolution of atom–atom negativity for $\Omega=0.1\,g$. (a) $\bar{n}=20$, (b) $\bar{n}=40$ and when the atoms are initially prepared in $|\Psi_1(0)\rangle=|+\rangle$ and $|\Psi_2(0)\rangle=|-\rangle$ (dotted), $|\Psi_1(0)\rangle=\frac{1}{\sqrt{2}}(|+\rangle+|-\rangle)$ and $|\Psi_2(0)\rangle=\frac{1}{\sqrt{2}}(|+\rangle-|-\rangle)$ (solid).

also show that ETA increases with the increase of the relative phase $\Delta\varphi(\Delta\varphi = |\varphi_2 - \varphi_1|)$ of the two initial coherent states for the case considered in this paper, which means that ETA depends not only on the initial atomic states and the mean photon number but also on the relative phase $\Delta\varphi$ of the two initial atomic coherent states.

Figure 2 displays how the evolution of ETA depends on the coupling constant for $\bar{n} = 20$. From these figures, we find that ETA revealed by the solid lines is stronger than that by the dotted lines at most time. The value of atom–atom negativity is larger when the dipole interaction between the atoms is involved (as shown in Figs.2(b) and 2(c)) than that when the dipole interaction between the atoms is absent (as shown in Fig.2(a)). The evolution of ETA is approximately periodic for $\Omega \neq 0$ (Figs.2(b) and 2(c)), and the period shortens with the increase of coupling constant.

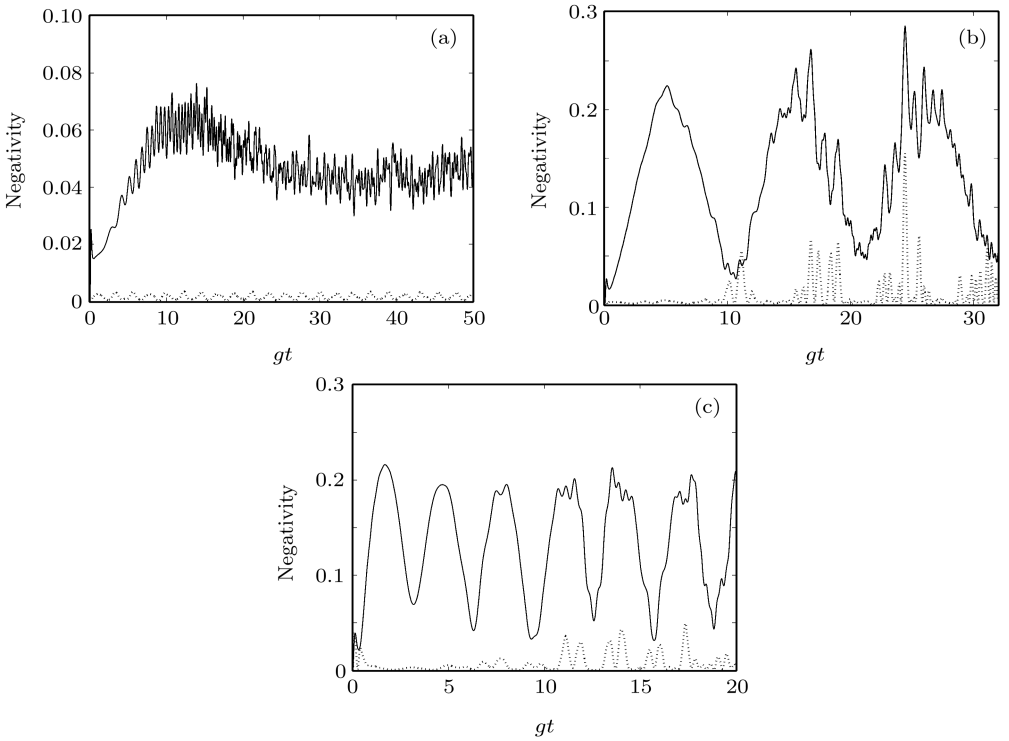


Fig.2. The evolution of atom–atom negativity for $\bar{n} = 20$. (a) $\Omega = 0$, (b) $\Omega = 0.3\,g$ and (c) $\Omega = 1.0\,g$ when the atoms are initially prepared in $|\Psi_1(0)\rangle = |+\rangle$ and $|\Psi_2(0)\rangle = |-\rangle$ (dotted), $|\Psi_1(0)\rangle = \frac{1}{\sqrt{2}}(|+\rangle + |-\rangle)$ and $|\Psi_2(0)\rangle = \frac{1}{\sqrt{2}}(|+\rangle - |-\rangle)$ (solid).

3.2. The entanglement between the two atoms in $|\Psi(0)\rangle = C|+-\rangle + \sqrt{(1-C^2)}\mathrm{e}^{\mathrm{i}\varphi}|-+\rangle$

Here C is the real coefficient and φ is the relative phase. It should be noticed that the two atoms are initially entangled when $C \neq 1$ or 0 and maximally entangled when $C = \frac{1}{\sqrt{2}}$. The initial density matrix for the two atoms can be expressed as

$$\rho_{\mathrm{a}}(0) = \begin{pmatrix} 0 & 0 & 0 & 0 \\ 0 & C^2 & C\sqrt{1-C^2}\mathrm{e}^{-\mathrm{i}\varphi} & 0 \\ 0 & C\sqrt{1-C^2}\mathrm{e}^{\mathrm{i}\varphi} & 1-C^2 & 0 \\ 0 & 0 & 0 & 0 \end{pmatrix}. \quad (8)$$

We can obtain the density matrix of the two atoms at time t when we substituting Eqs.(2) and (8) into Eq.(4):

$$\rho_{\mathrm{a}}(t) = \begin{pmatrix} \rho_{11} & 0 & 0 & 0 \\ 0 & \rho_{22} & \rho_{23} & 0 \\ 0 & \rho_{23}^* & \rho_{33} & 0 \\ 0 & 0 & 0 & \rho_{44} \end{pmatrix}, \quad (9)$$

where the matrix elements are

$$\rho_{11} = \sum_n P_n \left[1 + C\sqrt{1-C^2}\left(\mathrm{e}^{-\mathrm{i}\varphi} + \mathrm{e}^{\mathrm{i}\varphi}\right)\right] n \left|\frac{B_n}{\Theta_n}\right|^2,$$

$$\rho_{22} = \sum_n P_n\{C^2|U_{22n}|^2 + (1-C^2)|U_{23n}|^2 + C\sqrt{1-C^2}(\mathrm{e}^{-\mathrm{i}\varphi}U_{22n}U_{23n}^* + \mathrm{e}^{\mathrm{i}\varphi}U_{23n}U_{22n}^*)\},$$

$$\rho_{23} = \sum_n P_n \Big\{ C^2 U_{22n} U_{23n}^* + C\sqrt{1-C^2}\mathrm{e}^{-\mathrm{i}\varphi}|U_{22n}|^2 + C\sqrt{1-C^2}\mathrm{e}^{\mathrm{i}\varphi}|U_{23n}|^2 + (1-C^2)U_{23n}U_{22n}^* \Big\},$$

$$\rho_{33} = \sum_n P_n \Big\{ C^2|U_{23n}|^2 + (1-C^2)|U_{22n}|^2 + C\sqrt{1-C^2}\mathrm{e}^{-\mathrm{i}\varphi}U_{23n}U_{22n}^* + C\sqrt{1-C^2}\mathrm{e}^{\mathrm{i}\varphi}U_{22n}U_{23n}^* \Big\},$$

$$\rho_{44} = 1 - \rho_{11} - \rho_{22} - \rho_{33}.$$

The numerical results of atom–atom negativity according to Eq.(9) are displayed in Figs.3 and 4. Figure 3 shows how the mean photon number $\bar{n}$ and the coefficient C affect ETA, while Fig.4 describes how the atom–atom negativity depends on the coefficient C and the relative phase φ. From these figures, we find the following: firstly, comparing the solid lines and the dashed lines with the dotted lines in every figure, we find that the atom–atom negativity of the two atoms in the initial coherent states is always larger than that of the two atoms initially in the pure initial states, which means the possibility that one can get strong entanglement between the two atoms by means of the initial atomic coherence; secondly, with the increase of coefficient C from 0 to $\frac{1}{\sqrt{2}}$, ETA is enhanced and becomes largest when $C = \frac{1}{\sqrt{2}}$. Finally, the influence of the relative phase on the entanglement can be observed from Fig.4. It is clear that, with the increase of relative phase from 0 to π (corresponding to the dotted, dashed and solid lines in the figures), the ETA increases. When $\varphi = 0$ the two atoms are disentangled at some specific times, while when $\varphi \neq 0$ the two atoms are entangled at all time. In addition, from Fig.4(a), we find that the atom–atom negativity becomes larger than its initial value for $\varphi = \frac{2}{3}\pi$ and $\varphi = \pi$, which means that ETA can be amplified by changing appropriate initial parameters of the system.

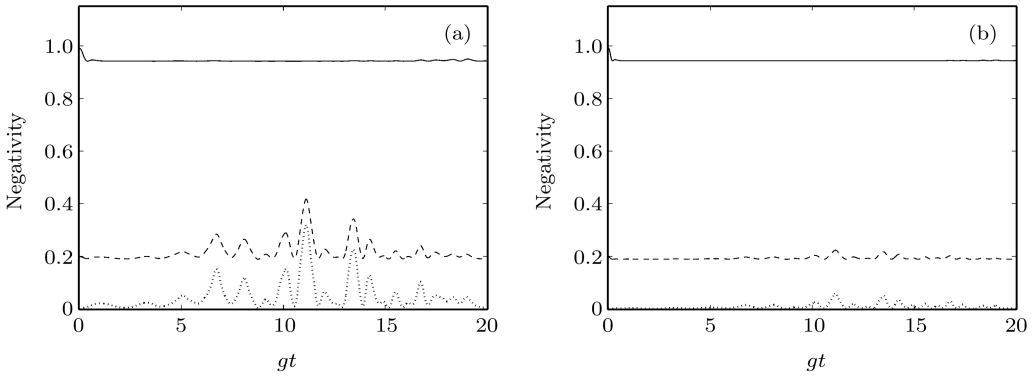


Fig.3. The evolution of atom–atom negativity induced by interacting with a thermal field for $\Omega = 0.1\,g$ (a) $\bar{n} = 5$, (b) $\bar{n} = 20$ when the atoms are initially prepared in $|\Psi(0)\rangle = |+-\rangle$ (dotted), $|\Psi(0)\rangle = 0.1|+-\rangle + 0.9950\mathrm{e}^{\mathrm{i}\frac{9}{10}\pi}|-+\rangle$ (dashed) and $|\Psi(0)\rangle = \frac{1}{\sqrt{2}}(|+-\rangle + \mathrm{e}^{\mathrm{i}\frac{9}{10}\pi}|-+\rangle)$ (solid).

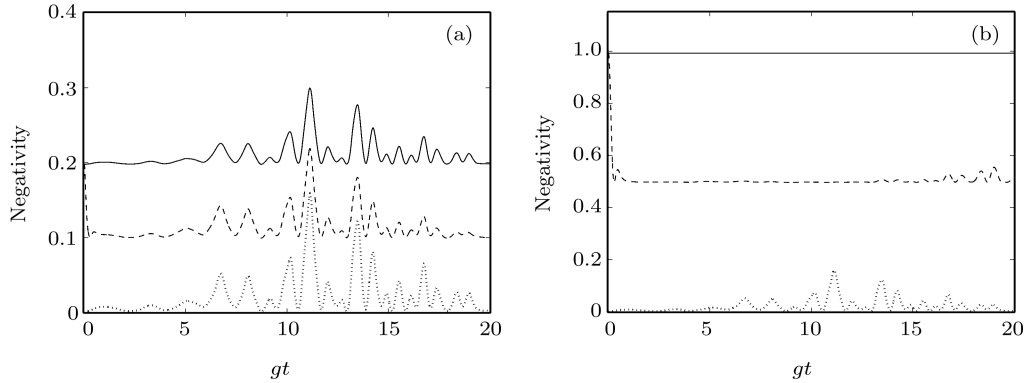


Fig.4. The evolution of atom–atom negativity induced by interacting with a thermal field for $\bar{n} = 10$, $\Omega = 0.1\,g$ and (a) $C = 0.1$ (b) $C = 1/\sqrt{2}$ and the relative phases are $\varphi = 0$ (dotted), $\varphi = \frac{2}{3}\pi$ (dashed) and $\varphi = \pi$ (solid).

4. Conclusion

In this paper, we have studied the entanglement properties in a system of two dipole–dipole coupled two-level atoms resonantly interacting with a single-mode thermal field. We have calculated the negativity in order to quantify the atom–atom entanglement. The results show that, when the value of the mean photon number is very large (corresponding to high temperature), the dynamical entanglement is greatly enhanced due to the initial atomic coherence. These results are helpful for controlling the atomic entanglement by changing the initial parameters of the system, such as the superposition coefficients and the relative phases of the initial atomic coherent state, the coupling constant of the dipole interaction between the atoms and the mean photon number of the cavity field.

References

[1] Nilesen M A and Chuang I L 2000 *Quantum Computation and Quantum Information* (Cambridge: Cambridge University Press)

[2] Bennett C H, Brassard G and Vepeau C 1993 *Phys. Rev. Lett.* **70** 1895

[3] Bennett C H and Wiesner S J 1992 *Phys. Rev. Lett.* **69** 2881

[4] Ekert A 1991 *Phys. Rev. Lett.* **67** 661

[5] Korbicz J K, Cirac J I and Lewenstein M 2005 *Phys. Rev. Lett.* **95** 120502

[6] Plenio M B and Huelga S F 2002 *Phys. Rev. Lett.* **88** 197901

[7] Bose S, Jacobs K and Knight P L 1999 *Phys. Rev.* A **59** 3204

[8] Abdel-Aty Mahmoud, Wahiddin M R B and Obada A-S F 2005 quant-ph/0503106

[9] Tanas R and Ficek Z 2004 *J. Opt.* B: *Quantum Semiclass. Opt.* **6** S610

[10] Wu Y, Payne M G, Hagley E W and Deng L 2004 *Phys. Rev.* A **70** 063812

[11] Tanaś R and Ficek Z 2004 *J. Opt.* B: *Quantum Semiclass. Opt.* **6** S90

[12] Malinovsky V S and Sola I R 2004 *Phys. Rev. Lett.* **93** 190502

[13] Gu S J and Lin H Q 2005 quant-ph/0503132

[14] Fu H, Wang X and Solomon A I 2001 *Phys. Lett.* A **291** 73

[15] Wu Q, Fang M F and Hu Y H 2007 *Chin. Phys.* **16** 1971

[16] Hu Y H,Fang M F and Liao X P 2007 *Chin. Phys.* **16** 1344

[17] Scully M O and Zubairy M S 1997 *Quantum Optics* (Cambridge: Cambridge University Press)

[18] Scully M O 1985 *Phys. Rev. Lett.* **55** 2802

[19] Scully M O and Zubairy M S 1987 *Phys. Rev.* A **35** 752

[20] Zhu S Y 1996 *Phys. Rev. Lett.* **76** 388

[21] Huang H, Zhu S Y and Zubairy M S 1997 *Phys. Rev.* A **55** 744

[22] Leviatan A and Shao B 1990 *Phys. Rev. Lett.* **64** 110

[23] Li F L, Xiong H and Zubairy M S 2005 *Phys. Rev.* A **72** 010303(R)

[24] Wang X Y, Du S D and Chen X S 2006 *J. Phys.* B **39** 3805

[25] Hu Y H, Fang M F and Wu Q 2007 *Chin. Phys.* **16** 2407

[26] Bose S, Fuentes-Guridi I, Knight P L and Vedral V 2001 *Phys. Rev. Lett.* **87** 050401

[27] Kim M S, Lee J, Ahn D and Knight P L 2002 *Phys. Rev.* A **65** 040101

[28] Aguiar L S, Munhoz P P, Vidiella-Barranco A and Roversi J A 2005 *J. Opt.* B: *Quantum Semiclass. Opt.* **7** S769

[29] Zhou L, Song H S and Li C 2002 *J. Opt.* B: *Quantum Semiclass. Opt.* **4** 425

[30] Zhou L, Yi X X, Song H S and Quo Y Q 2004 *J. Opt.* B: *Quantum Semiclass. Opt.* **6** 378

[31] Bashkirov E K 2006 *Laser Phys. Lett.* **3** 145

[32] Peres A 1996 *Phys. Rev. Lett.* **77** 1413

[33] Horodecki P 1997 *Phys. Lett.* A **232** 333

[34] Plenio M B and Virmani S 2005 quant-ph/0504163